RUHUNA JOURNAL OF SCIENCE
Vol 16 (2): 43-55, December 2025
eISSN: 2536-8400
http://doi.org/10.4038/rjs.v16i2.155



Faculty of Science
University of Ruhuna

Modelling and simulation of miscible fingering instability in a two-phase system with gravity: Application to oil recovery enhancement

C.W. Sahabandu[*1] and M. Dewasurendra[2]

[1] *Department of Mathematics, The Open University of Sri Lanka, Nugegoda, Sri Lanka*
[2] *Department of Mathematics, University of Peradeniya, Peradeniya, Sri Lanka*

*Correspondence: cwsah@ou.ac.lk, ORCID: https://orcid.org/0000-0002-5940-6908

Received: 27th May 2025, Accepted: 23rd November 2025, Published: 31st August 2026

Abstract Enhanced oil recovery (EOR) processes rely heavily on understanding the complex behaviour of miscible and immiscible fingering, particularly under the influence of gravity, as fingering instability can significantly affect fluid displacement in two-phase systems. This study used COMSOL Multiphysics to investigate miscible fingering instability in a two-phase system affected by gravity, and included the gravitational effects in the computational model in order to take account of their influence on fluid flow dynamics. The dynamic interaction between miscible fluids was studied in order to clarify the mechanisms responsible for fingering instability and its effect on displacement efficiency. Moreover, the spatiotemporal evolution of species concentration and miscible fluid saturation was recorded in order to assess the displacement behaviour of the different injected fluids. The results highlight key benefits of miscible EOR, including improved sweep efficiency, reduced mobility ratio sensitivity, and enhanced displacement efficiency. Findings were consistent with previous investigations, and the simulations showed that nano-brines achieved higher oil recovery than carbonated water. Among the nano-agents tested, aluminium oxide performed most effectively, followed by silicon dioxide and magnesium oxide. Oil production is highly dependent on both the inclination angle and the dip direction, while this study concluded that gravity plays a significant role in inclined reservoirs, strongly influencing fluid flow behaviour.

Keywords: COMSOL Multiphysics, Enhanced oil recovery, Gravity effect, Miscible fingering instability

1 Introduction

Miscible displacement is a crucial phenomenon with widespread implications across various fields including oil recovery, contaminant transport in aquifers, chromatography separation, and numerous environmental and industrial processes. The displacement of a high-viscous fluid by a low-viscous fluid in porous media or Hele-Shaw cells (Saffman and Taylor 1958) often leads to a hydrodynamic instability known as viscous fingering. This instability observed in both miscible and immiscible fluids manifests as the growth of perturbations at the fluid interface due to differences in the

mobility of interacting fluids. While Darcy's law (Chen 2007) is conventionally employed for momentum conservation in porous media, its application has limitations (Homsy 1987, Pramanik *et al*. 2012), particularly in cases of large fluid velocities and significant viscous shear effects, where non-Darcian behaviour becomes apparent (Kumar *et al*. 2016). However, this paper focused only on the Darcian flow fields. In the realm of computational modelling, several approaches have been developed to simulate miscible viscous fingering, primarily based on Darcy's law (Homsy 1987, Székely 2018). These include equation-based models such as the framework proposed by Holzbecher (2009) that couples Poisson and convection-diffusion equations, and models based on Two-Phase Darcy's Law employed by Pramanik *et al*. (2012). However, these models are typically confined to describing viscous fingering instabilities solely in a Darcian porous medium.

Physical and mathematical description of the fingering

Darcy's law is a fundamental principle in the study of one-phase fluid flow through a porous medium with lower porosity (Chen 2007). Henry Philibert Gaspard Darcy, a French hydraulic engineer, conducted experiments with a water tank, leading to the discovery of a relationship between the flow rate and the pressure difference (Chen 2007). Darcy flux is often called the velocity, although it differs from microscopic velocity. It represents the volumetric flow rate per unit of the total cross-sectional area of the porous medium, accounting for the blocked areas caused by materials like sand or rocks. This macroscopic velocity is calculated based on the Representative Elementary Volume (REV) discussed in Székely 2018.

Darcy's law (Darcy 1856) can be expressed as,

$$\underline{u} = -\frac{Kk}{\mu(c)}(\nabla p - \rho g \sin\alpha)$$

This equation relates the seepage velocity $\underline{u}$ to the pressure gradient ∇p, considering the gravitational force $\rho g \sin\alpha$, permeability K and the relative permeability k of the porous medium. It essentially reflects the conservation of momentum, and it can be derived from the Navier-Stokes equations (Constantin and Foias 1992).

The saturation of injective fluid refers to the proportion or percentage of the reservoir rock's pore space that is occupied by the injected fluid (e.g. water, miscible/ immiscible gases, nano or biomaterials, polymer/ clay particles) during the EOR process. Increasing the saturation of the injective fluid can contribute to EOR in several ways (Buckley and Leverett 1942). It improves fluid mobility, reduces residual oil saturation, enhance sweep efficiency while minimizing bypassed oil, interfacial tension reduction, and miscibility enhancement. In some cases, particularly in gas injection methods like CO_2 flooding, increasing the saturation of the injective fluid can enhance the miscibility with oil. This promotes improved oil displacement by reducing oil viscosity and swelling the oil phase (Sahabandu *et al*. 2025).

In the context of fluid flow through a porous medium, saturation S_i is a key parameter that defines the portion of a porous medium occupied by a specific phase i (wetting or non-wetting phase). Assuming that the fluids completely fill the void space between

rocks. This leads to a fundamental relation of saturation, as given by,

$$\sum_i S_i = 1$$

This equation signifies that the saturation of a particular phase is equal to 1, indicating complete filling of the void space (Pramanik *et al*. 2012). Although the saturation of any phase theoretically ranges from 0 to 1, in the practical scenarios, once water reaches the irreducible water saturation, it becomes immobile (Székely 2018).

When it comes to immiscible fluids, they are separated by a clear and infinitely thin boundary which has surface tension. The value of surface tension is the measure of the forces needed to alter the shape of the interface, and the system always tends to reduce its surface energy. As a result, the interface of a droplet within another phase tends to assume a spherical shape, and the interface tension keeps the phases apart, regardless of the droplet's size. The flow dynamics are significantly influenced by how the phases attach to the solid material's interface, such as rock. The ability of a liquid to maintain contact with a solid interface is termed wettability, and it is determined by adhesive forces when the liquid and solid are in contact. These intermolecular forces cause water droplets to spread across the mineral surface. In cases where both phases are present in a pore, one may be more attracted to mineral particles, leading to the classification of the system as either water-wet or non-wet.

When the phases are wetting or non-wetting, the relationship between the contact angle θ and the interface energies can be expressed using the Young's equation (Székely 2018):

$$\cos\theta = \frac{\gamma_{os} - \gamma_{ws}}{\gamma_{ow}}$$

Here, the subscripts s and γ refer to the solid and the surface energy, respectively. The contact angle less than 90 degrees, is more commonly observed in nature and the porous medium is referred to as hydrophilic.

In EOR, the terms wetting and non-wetting phases describe the way fluids behave in a porous rock when interacting with the solid surfaces. They indicate the degree to which fluids, generally oil and water, are attracted to the rock surfaces and affect the process of displacing and recovering oil from the reservoir (Beteta *et al*. 2024). The wetting phase is the fluid which has a stronger attraction to the solid surfaces of the porous rock; it is the one that spreads out and wets the rock surfaces, thereby establishing better contact with the reservoir rock. For instance, in the case of water-wet systems, water is regarded as the wetting phase since it wets the rock surfaces more than oil. The non-wetting phase is the fluid that has a weaker affinity or attraction to the solid surfaces of the porous rock.

The characteristics of wetting and non-wetting are important in EOR processes, such as water flooding or polymer flooding, since the aim is to displace and recover more oil from the reservoir. Understanding wetting properties helps develop strategies to improve displacement efficiency and the total amount of oil recovered. The selection of the appropriate EOR methods and the injection of particular fluids (for example, water, gas, nano fluids, or polymers) will depend on whether the reservoir is water-wet or oil-wet, as this influences the way fluids travel through the porous rock and the displacement of the oil that is trapped (Székely 2018, Beteta *et al*. 2024).

In single-phase models, permeability K is a key parameter determining the rate at which a fluid flows through a porous medium, and it is known as absolute permeability and measures the medium's ability to transmit the fluid (Wyckoff and Botset 1936). Although it is in theory an intrinsic property, interactions at the microscale between the rock and the fluid can affect the permeability. Moreover, unlike liquids, gases do not satisfy the no-slip condition at the microscale and thus have different interactions with the rock surface. In the multiphase flow system, each phase i exhibits an effective permeability K_i^{eff}, which is always smaller than the absolute permeability K. This stems from the inherent capillary pressure in immiscible fluid flows, where a fluid must overcome this pressure to displace another fluid. Therefore, the relationship is expressed as,

$$\sum_i K_i^{eff} < K$$

To properly model this phenomenon, a new property termed as relative permeability k_i is introduced. It is defined as the ratio of the effective permeability for a specific phase to the absolute permeability of the porous medium (Székely 2018).

$$k_i = \frac{K_i^{eff}}{K} \text{ and } K_i^{eff} = k_i K$$

The gravitational forces acting on the fluids introduce additional challenges to the phenomenon, thereby necessitating a comprehensive investigation (Sahabandu *et al*. 2025). This research employed advanced modelling and simulation techniques to investigate the behaviour of miscible fingering in a two-phase system under the gravitational field, while additionally exploring the impact of the oil-layer elevation direction on recovery efficiency using computational fluid dynamics. This aspect is crucial for understanding how the spatial distribution of fluids within a porous medium affects displacement performance. Furthermore, the study demonstrates detailed flow visualizations of the fingering phenomenon. Although Sahabandu *et al*. (2021, 2025) reported numerical findings using similar injected fluids under comparable conditions, those studies lacked direct flow visualizations to support their interpretations. Addressing this gap, the present study incorporates COMSOL based flow behaviour analysis to visually interpret and validate the dynamics of miscible displacement, thereby strengthening the physical understanding of fingering mechanisms. By analyzing variations in oil recovery under different elevation configurations and presenting visual evidence of the flow dynamics, this work provides additional information for developing optimization strategies in EOR techniques. The study contributes a novel and valuable perspective to the field of EOR, supporting the development of more efficient approaches for extracting heavy oil from subsurface reservoirs.

2 Methods

In this research, a homogeneous and isotropic porous material with permeability K and constant porosity $\epsilon_p$was considered. As shown in Figure 1, the geometry consists of a

horizontal rectangular domain of length L_x, width L_y with injective fluid speed U. It was assumed that the solute dispersion in the porous medium is isotropic and that x_0 represents the interface position with thin transition zone δ. All the injective fluids were assumed to be incompressible, buoyantly neutral, and miscible.

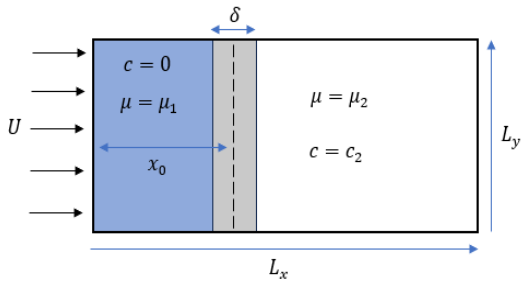


Fig 1. Schematic diagram of displacement of miscible fluid in 2D homogeneous porous medium

2.1 Two Phase Darcian Domain

Without loss of generality, an injective fluid was considered with a viscosity of μ_1 and a solute concentration of $c = 0$ mol m^{-3}, whereas native fluid had a viscosity of μ_2 and a solute concentration of $c = c_2$ mol m^{-3} in the solvent. Simulations were initiated by assuming that the injective fluids are miscible because this causes a thin transition zone between the two phases to form right away and denoted thickness of that as δ. At x_0, the interfacial concentration was given as $c = \frac{c_2}{2}$ mol m^{-3}.

To form a more advanced model, the density of the injective fluid and native fluid was denoted by ρ_1 and ρ_2 respectively. Assuming that the porous medium was fully saturated, $s_1 + s_2 = 1$, where s_1 and s_2 represented the saturations of the injective and native fluids, respectively. For this scenario, the two-phase Darcy's law in COMSOL Multiphysics was considered. The pressure gradient was the only component at the current position that generates fluid flow. The equation of continuity can be expressed as,

$$\nabla \underline{u_i} = 0; \quad i = 1, 2 \tag{1}$$

By Darcy law,

$$\nabla p_i = -\frac{\mu_i(c)}{K\, k_i} \underline{u_i} \tag{2}$$

where k_i was the relative permeability. The boundary conditions associated with the equations (1) and (2) were

$$\underline{u_i} = (U, 0) \quad \text{and} \quad c = 0 \text{ at } x = 0 \tag{3}$$

$$p = 0 \quad \text{at} \quad x = L_x \tag{4}$$

$$\frac{\partial u_i}{\partial x} = 0,\ v = 0 \quad \text{at} \quad y = 0 \text{ and } y = L_y \tag{5}$$

From the convection-diffusion equation, the transfer of solute concentration could be expressed as

$$\varepsilon_p \frac{\partial c}{\partial t} + \underline{u_i} \cdot \nabla c = \varepsilon_p D \nabla^2 c \tag{6}$$

The boundary conditions associated with the equation (6) were

$$c = 0 \quad \text{at} \quad x = 0 \tag{7}$$
$$\frac{\partial c}{\partial x} = 0 \quad \text{at} \quad x = L_x \tag{8}$$
$$\frac{\partial c}{\partial y} = 0 \quad \text{at} \quad y = 0 \quad \text{and} \quad y = L_y \tag{9}$$

Equations (1), (2) and (6) made up the entire governing system of equations, where $\underline{u_i} = (u, v)$, p, $\mu(c)$, D are the two-dimensional Darcy (or seepage) velocity vector, dynamic pressure, the dynamics viscosity of the fluid which depends on the concentration of the fluid, molecular diffusion coefficient.
Assuming the relation to be monotonic,

$$\mu_i(c) = \mu_i \exp(Rc); \quad i = 1, 2 \quad \text{where } R = ln\left(\frac{\mu_2}{\mu_1}\right) \tag{10}$$

is the log-mobility ratio. Since a transition region is of δ exist between the two fluids, the initial condition for concentration is given by,

$$c(x, y, 0) = \frac{c_2}{2}\left[1 + \text{erf}\left(\frac{x - x_0}{\delta}\right)\right] \tag{11}$$

where "erf" stands for the error function, $\text{erf}(x) = \int_0^x e^{-\frac{z^2}{2}} dz$

2.2 Two phase Darcian Domain under gravitational effect

In EOR simulations conducted within the elevation domain using COMSOL, gravity becomes a pivotal factor, requiring a modification to the Darcy equation to accurately capture the interplay between fluid flow and gravitational forces. The conventional Darcy equation, which characterizes fluid flow through a porous medium is augmented to account for gravity, particularly when elevation changes significantly affect flow dynamics. This modification acknowledges that gravitational forces contribute to the overall pressure gradient, influencing fluid movement in porous formations.

COMSOL enables the incorporation of such gravity-dependent modifications into the simulation framework. So, proposed modelling approach allows for a better understanding of fluid behaviour in the reservoir, particularly when considering elevated regions where gravitational effects play a crucial role in governing the displacement and distribution of oil within the porous matrix. Consequently, integrating gravity-induced modifications into the Darcy equation in COMSOL simulations provides a more accurate representation of EOR processes, aiding the optimization and design of strategies for efficient oil recovery in diverse geological scenarios (Figure 2).

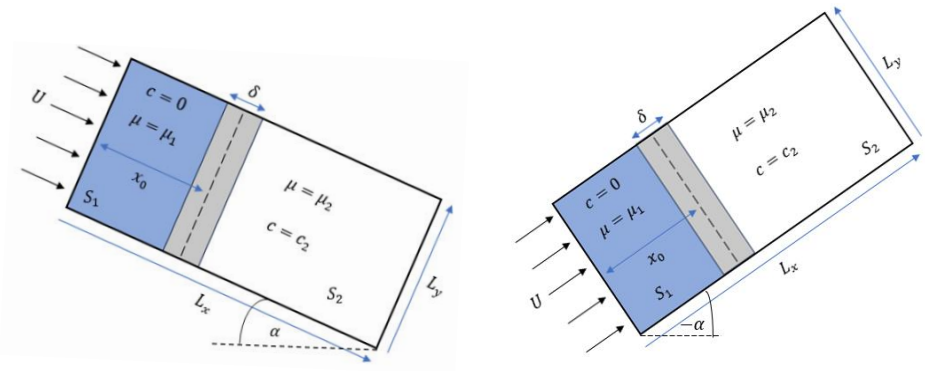


Fig 2. Schematic diagrams of displacement of miscible fluid in 2D homogeneous porous medium with an elevation

For miscible fingering, the Darcy law becomes accounting for gravitational impact as

$$\underline{u_i} = -\frac{Kk_i}{\mu_i(c)}(\nabla p - \rho_i g \sin\alpha) \tag{12}$$

where α is the angle of the elevation, which was measured in the negative x-direction, and it could be expressed as

$$\underline{u_i} = -\frac{Kk_i}{\mu_i(c)}(\nabla p + \rho_i g \sin\alpha) \tag{13}$$

when it is inclined to the positive $x-$direction, making a similar angle. The initial condition for concentration was

$$c(x,y,0) = \frac{c_2}{2}\left[1 + \text{erf}\left(\frac{x\cos\alpha - x_0}{\delta}\right)\right] \tag{14}$$

While numerous COMSOL studies have investigated Darcian miscible fingering (Pramanik *et al*. 2012, Holzbecher 2009), a notable gap exists in addressing the effects of different densities between the injective and native fluids, as well as the presence of an inclined oil layer. These factors introduce significant complexities that can substantially influence the dynamics of miscible displacement processes in porous media. The density contrast between the injected and the native fluids can lead to buoyancy-driven effects, altering flow patterns and fluid distribution within the porous medium. Moreover, an inclined oil layer introduces additional gravitational forces that can further affect the displacement process and subsequent recovery efficiency (Figure 2).

Despite the importance of these factors, existing studies have largely overlooked their contributions, focusing primarily on simpler scenarios without considering density variations or inclined oil layers. The effects of density contrasts and inclined oil layers into the modelling framework were incorporated, and this approach more accurately represents real-world scenarios and enhances the understanding of the underlying mechanisms governing miscible displacement processes in porous media. In this study, various domains were explored, including vertical upwards, vertical downwards, and inclined orientations towards both the negative and positive x-directions.

3 Results and Discussion

Equation (1) represents the conservation of mass under the assumptions of constant porosity and fluid density, with no additional mass sources in the system. At the inlet, the normal inflow velocity is prescribed, while the outlet boundary is assigned a specified pressure. The transverse boundaries are subject to a no-flow condition. To discretize the domain, a detailed triangular mesh was utilized for fluid dynamics, as illustrated in Figure 3. This meshing approach introduces triangular disruptions at the fluid interface, facilitating an accurate depiction of the intricate geometries and fluid behaviour within the homogeneous Darcy porous medium.

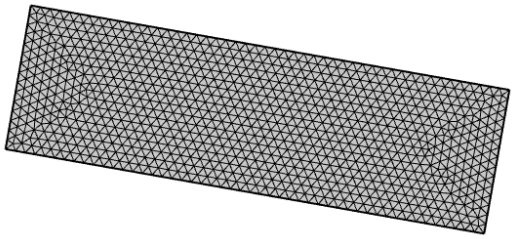


Fig 3. Computational domain and mesh used for the numerical simulations when $\alpha = 10^{\circ}$

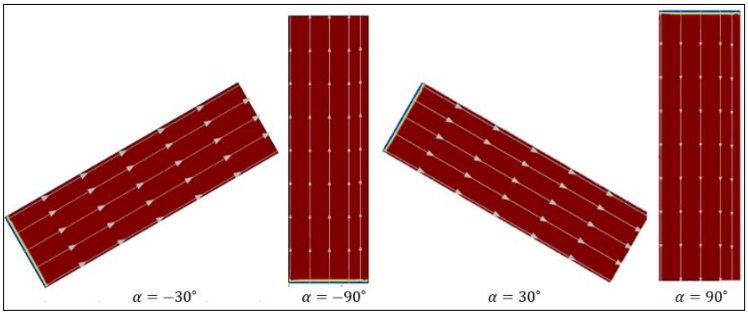


Fig 4. Initial distribution of fluids at $T = 0$ for different elevations

Spatio-temporal evolution of the species concentration were captured for miscible fluids at certain times, $T = 20$ s and $T = 50$ s, with the use of parameter values from the existing literature given in the Table 1 when accounting for elevations $\alpha = -30^{\circ}, -90^{\circ}, 10^{\circ}, 30^{\circ}$, and 90° for $U = 1 \times 10^{-3}$ ms^{-1}. Aluminum oxide has a higher saturated fingers formation whereas carbonated water injection had lower saturated fingers compared to others at any elevation or time (Figures 5 to 9).

The correlation between injective fluid saturation and native fluid (oil) saturation within the porous medium was a critical aspect of this study. As the saturation of the injective fluid was increased, there was a corresponding decrease in the saturation of the native fluid, ultimately resulting in the recovery of the trapped oil portion within the domain (since $S_1 + S_2 = 1$). Accordingly, manipulating the injection fluid saturation may be a key strategy for the recovery of heavy oil in EOR processes. To elucidate the

saturation effects, several influencing factors were systematically examined, including gravitational force, angle of elevation, injection direction, miscibility, and mobility ratio. The results presented in Figures 5 to 10 revealed that an increase in injective fluid saturation, coupled with optimized values of other parameters, leads to a more effective displacement of heavy oil, enhancing overall recovery efficiency.

Table 1: Physical and model parameters used in the simulations

Parameter	Symbol	Value and Unit			
Length of domain	L_x	1 m			
Width of domain	L_y	0.3 m			
Injection Speed	U	10^{-3} ms^{-1}			
Initial saturation	s_1	.001			
Initial pressure	p	0			
Gravitational acceleration	g	9.8 ms^{-2}			
Diffusion coefficient	D	4×10^{-8} m^{2}s^{-1}			
Interface position	x_0	0.01 m			
Thickness of the transition zone	δ	10^{-4} m			
Porosity	ϵ_p	0.1			
Permeability	κ	10^{-12} m^2			
Native fluid density	ρ_2	899 Kgm^{-3}			
Native fluid viscosity	μ_2	19 mPa. s			
Miscible brines		Al_2O_3	SiO_2	MgO	CO_2
Injective fluid density	ρ_1 [Kgm^{-3}]	1013	1012	968	1010
Log-mobility ratio	R	2.8	2.9	3.1	3.3

Additionally, results demonstrate that when employed as injection fluids, nano-brines yield superior oil recovery compared to alternative methods (Djebour *et al.* 2014, Neild and Bejan 1992, Prajapati and Desai 2016, Sahabandu *et al*. 2025). Notably, aluminium oxide is the most effective, followed by silicon dioxide and magnesium oxide, respectively (Figures 5-9) (Sahabandu *et al*. 2025). Furthermore, these findings indicate that employing a high-viscosity injective fluid with the augmenting the angle of elevation (but depend on the direction) can significantly enhance the efficiency of oil recovery (Figures 5-9) (Sahabandu *et al*. 2025).

Moreover, a gradual increase in the saturation of nano-brine within the considered domain was observed as the elevation shifted toward the negative x-direction, including vertically downward movements. Conversely, saturation decreases with elevation towards the positive x-direction, including vertically upward movements (Figure 10). This phenomenon leads to increased oil recovery with downward elevation and reduced oil recovery with upward elevation, primarily due to gravitational effects (Figures 5-10).

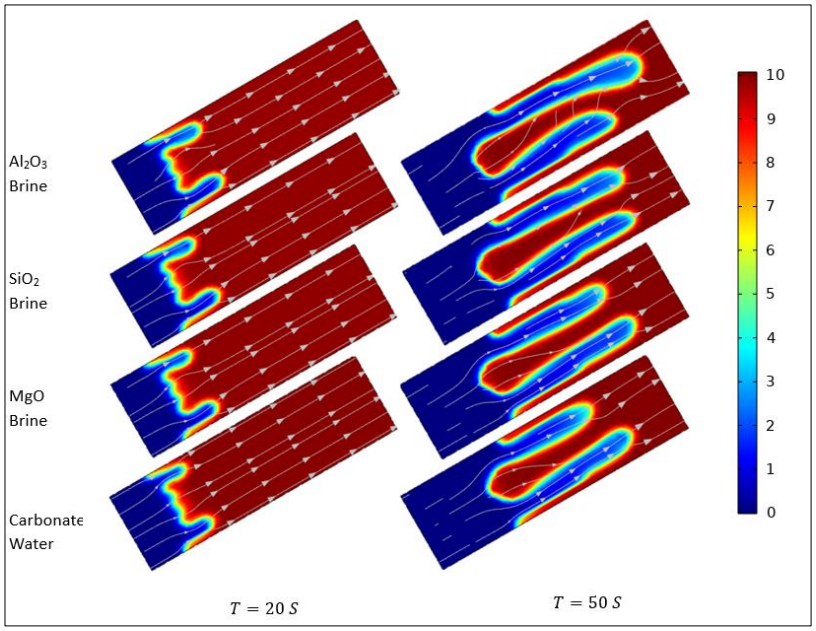


Fig 5. Spatio-temporal evolution of the species concentration of miscible fluids for $T = 20$ s and $T = 50$ s when $\alpha = -30^{\circ}$

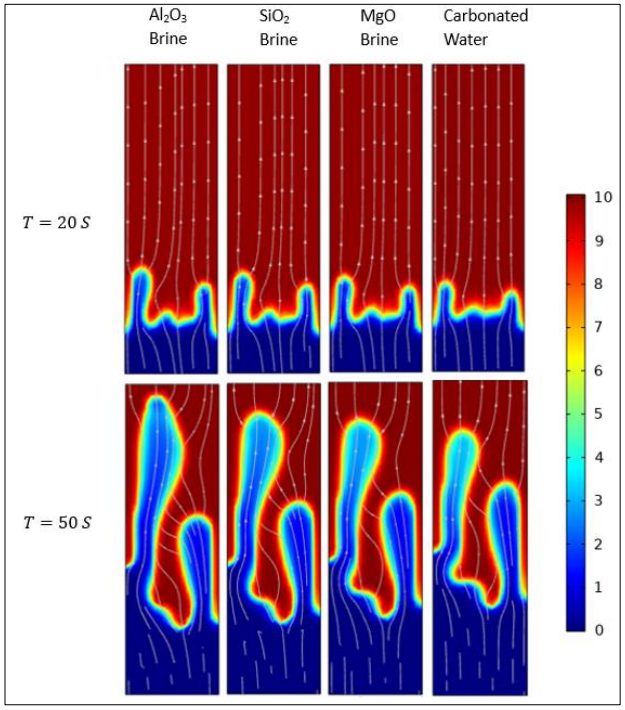


Fig 6. Spatio-temporal evolution of the species concentration of miscible fluids for $T = 20$ s and $T = 50$ s when $\alpha = -90^{\circ}$

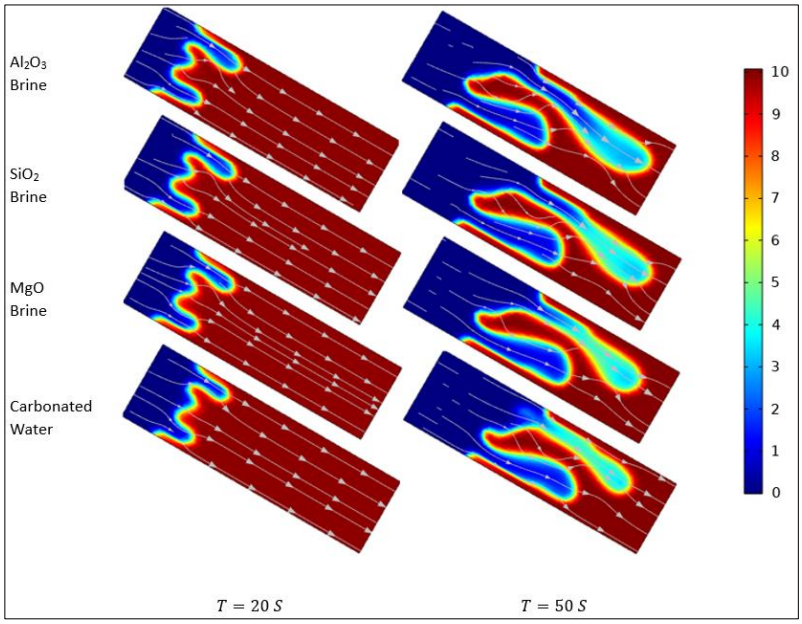


Fig 7. Spatio-temporal evolution of the species concentration of miscible fluids for $\mathbf{T = 20}$ s and $\mathbf{T = 50}$ s when $\boldsymbol{\alpha = 10^{\circ}}$

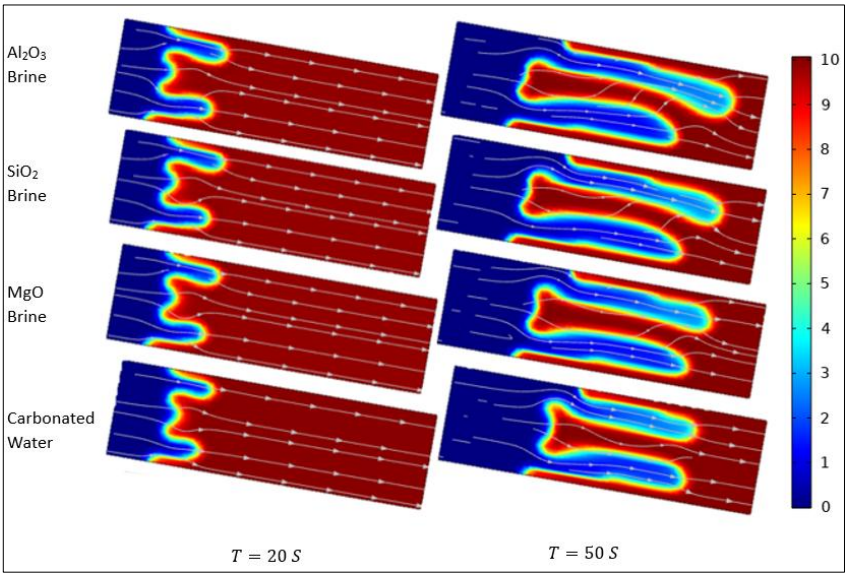


Fig 8. Spatio-temporal evolution of the species concentration of miscible fluids for $\boldsymbol{T = 20}$ s and $\boldsymbol{T = 50}$ s when $\boldsymbol{\alpha = 30^{\circ}}$

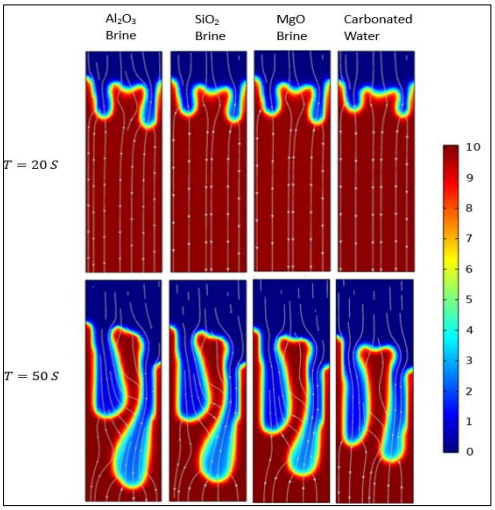


Fig 9. Spatio-temporal evolution of the species concentration of miscible fluids for $T = 20$ s and $T = 50$ s when $\alpha = 90°$

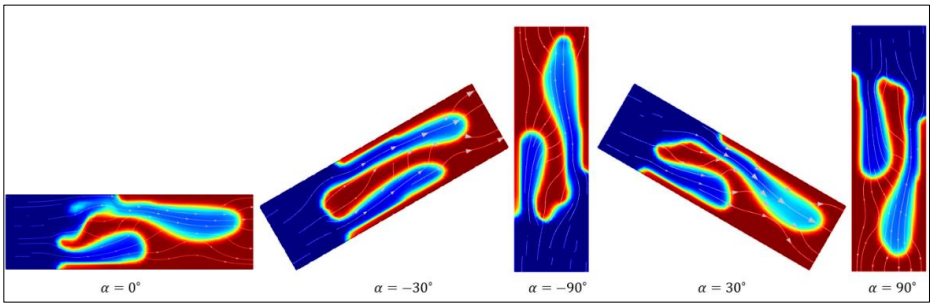


Fig 10. Spatio-temporal evolution of the species concentration of Al_2O_3 brine at $T = 50$ s for different elevations

4 Conclusions

This study extends the knowledge of in the field of EOR, offering information that can help in the design and implementation of more effective and sustainable strategies for maximizing heavy oil extraction from subsurface reservoirs. The accuracy and reliability of the results depend on the validity of the underlying models, assumptions, and input parameters. At intervals of $T = 20$ s and $T = 50$ s, the spatiotemporal distribution of the species concentration representing miscible fluid saturation was captured and analyzed for each injected fluid. The results show that the displacement behaviour changes with the type of injected fluid and the flow conditions. Furthermore, findings indicate that more oil can be extracted using nano-brines than using carbonated water. Aluminium oxide is the most common among them, followed by silicon dioxide and magnesium oxide, in that order. It can be concluded that gravity plays an important role in inclined oil layers, and oil production depends on both the layer's angle and the flow direction in agreement with numerical results from previous studies (Sahabandu *et al*. 2025).

Acknowledgements

RJS reviewers are acknowledged for critical comments to improve the initial manuscript for publication.

References

Beteta A, Sorbie KS, Skauge A, Skauge T. 2024. Immiscible viscous fingering: The effects of wettability/capillarity and scaling. *Transport in Porous Media* 151: 85–118. https://doi.org/10.1007/s11242-023-02034-z.

Buckley SE, Leverett MC. 1942. Mechanism of fluid displacement in sands. *Transactions of the AIME* 146(1): 107–116. https://doi.org/10.2118/942107-G

Chen Z. 2007. Reservoir Simulation: Mathematical Techniques in Oil Recovery. *CBMS-NSF Regional Conference Series in Applied Mathematics*, Vol. 77. Philadelphia, PA: Society for Industrial and Applied Mathematics (SIAM). DOI: 10.1137/1.9780898717075.

Constantin P, Foias C. 1992. Navier-Stokes equations. *Acts of Applied Mathematics* 28: 295–296. https://doi.org/10.1007/BF00047090.

Darcy H. 1856. Les fontaines publiques de la ville de Dijon: Exposition et application des principes à suivre et des formules à employer dans les questions de distribution d'eau. V. Dalmont.

Djebour H, Zouaout K, Mohammedi K, Aider AA. 2014. Viscous Fingering in Porous Media. *Advances in Computational Mechanics and Applications.* p 175.

Holzbecher E. 2009. Modeling of viscous fingering, *COMSOL conference*, Milan.

Homsy GM. 1987. Viscous Fingering in Porous Media. *Annual Review of Fluid Mechanics* 19(1):271–311. doi:10.1146/annurev.fl.19.010187.001415.

Kumar A, Pramanik S, Mishra M. 2016. COMSOL Multiphysics® Modeling in Darcian and Non-Darcian Porous Media*. Proceedings of the 2016 COMSOL Conference*, Bangalore, India. October 20-21. https://www.comsol.com/paper/modeling-darcian-and-non-darcian-porous-media-with-comsol-multiphysics-software-38691.

Neild DA, Bejan A. 1992. Convection in porous media. *Springer-Verlag*, Berlin. 5-14 edition.

Prajapati DJ, Desai NB. 2016. Application of the basic optimal homotopy analysis method to fingering phenomenon. *Global Journal of Pure and Applied Mathematics*. 12: 2011–2022 edition.

Pramanik S, Kulukuru GL, Mishra M. 2012. Miscible viscous fingering: Application in chromatographic columns and aquifers, *COMSOL conference*, Bangalore, India. November 1-2. https://www.comsol.com/paper/miscible-viscous-fingering-application-in-chromatographic-columns-and-aquifers-13539.

Saffman P, Taylor GI. 1958. The penetration of a fluid into a porous medium or Hele-Shaw cell containing a more viscous liquid. *Proceedings of the Royal Society of London. Series A. Mathematical and Physical Sciences* 245 (1242): 312–329. doi:10.1098/rspa.1958.0085.

Sahabandu CW, Karunarathna D, Sewvandi P, Juman ZAMS, Dewasurendra M, Vajravelu K. 2021. A Method of Directly Defining the inverse Mapping for a nonlinear partial differential equation and for systems of nonlinear partial differential equations. *Computational and Applied Mathematics* 40(6): 1-16. https://doi.org/10.1007/s40314-021-01627-y

Sahabandu CW, Dewasurendra M. 2024. COMSOL Multiphysics: CFD Simulations of Miscible and Immiscible Fingering Instability in Enhanced Oil Recovery*, International Conference on Computational and Mathematical Modelling.* 170-176.

Sahabandu CW, Juman ZAMS, Vajravelu K, Spangler B, Dewasurendra M. 2025. Modeling and semi-analytical solution for immiscible and miscible fingers formation during enhanced oil recovery, *International Journal of Modelling and Simulation* 45(5):1584-1595. https://doi.org/10.1080/02286203.2023.2296369.

Székely F. 2018. Mathematical modeling and numerical study of viscous fingering. MSc Thesis, *Department of Mathematics, Norwegian University of Science and Technology, NTNU* 1-59.

Wyckoff RD, Botset HG. 1936. The flow of gas-liquid mixtures through unconsolidated sands. *Physics* 7(9): 325–345. https://doi.org/10.1063/1.1745402